 https://doi.org/10.24191/jeesr.v28i1.005

Knee-Based Energy-Saving Measures Selection using MOPSO and NSGA-II

Siti Solehah Md Ramli[1] *, Mohammad Nizam Ibrahim [2], Anuar Mohamad @ Ahmad[3], Kamarulazhar Daud[4], Abdul Malek Saidina Omar[5], Nor Shuhada Ibrahim[6]

Abstract— **This paper benchmarks two Evolutionary Multi-Objective Optimization (EMO) methods, namely Multi Objective Particle Swarm Optimization (MOPSO) and Non-Dominated Sorting Genetic Algorithm II (NSGA-II), for selecting Energy-Saving Measures (ESMs) in an audited Malaysian academic building under a bi-objective trade-off between annual energy saving and investment cost, while avoided CO_2 is computed from energy saving using the fixed grid-emission factor as a carbon metric. For each algorithm, 30 seeds generate Pareto fronts in the cost–energy saving plane, shown in 2D for clear comparison, and the resulting carbon metric is visualized as a 3D projection. A curvature-based knee is extracted to yield one implementable package per run. Knee packages are valued over a 10-year horizon using Simple Payback Period (SPP), discounted Return on Investment (ROI), Life-Cycle Cost (LCC), and Savings-to-Investment Ratio (SIR) under fixed site assumptions. Relative to the auditor's package, the knee solutions cut Capital Expenditure (CAPEX) by approximately 87.3 % for MOPSO and 81.9 % for NSGA-II while sustaining around 21 % to 23 % of the auditor's annual energy savings and CO_2 avoidance. Economic performance improves markedly at the knees: SPP shortens to 2.25 yr for MOPSO and 3.54 yr for NSGA-II; discounted ROI rises to 235.24 % and 110.43 %; SIR increases to 3.18 and 2.03; and LCC is favorable at -RM 92,816 and -RM 62,614, respectively. Across 30 paired seeds, paired Wilcoxon tests indicate statistically and practically significant between-method differences at the knee, with the strongest separation in LCC and SPP. Overall, the MOPSO knee offers the strongest financial profile, whereas the NSGA-II knee attains slightly higher annual savings and CO_2 avoidance.**

Index Terms— **Building Energy Retrofits, Energy-Saving Measures, Knee Point, Life-Cycle Cost, MOPSO, NSGA-II.**

I. INTRODUCTION

Energy-Saving Measures (ESMs) and building retrofits are among the most effective levers for lowering operating costs and emissions in educational buildings and public facilities. Buildings and construction account for about one-third of global final energy use and energy-related CO_2, so retrofit choices must be transparent, auditable, and easy to justify [1]. Selecting which ESMs to implement is vital because it creates real trade-offs among investment cost, energy savings, and CO_2 avoidance. Multi-objective optimization fits this setting because it produces a Pareto front, which provides efficient options rather than a single result [2]-[10]. To keep carbon accounting consistent with Malaysian practice, avoided CO_2 is tied to energy saving via the national grid-emission factor and evaluated under standard M&V conventions [11], [12].

ESM selection from an audited catalogue is constrained by implementation and budgeting considerations. Facility teams typically need one defensible package that can proceed to procurement, rather than a long list of Pareto trade-offs. Audited portfolios often mix binary commitments such as awareness programmes, EMS, and BMS adoption with partial-coverage measures such as occupancy or sensor controls, lighting upgrades, and targeted VRF deployment. These mixed decision types, together with different caps and cost structures, create a mixed discrete–continuous search space. Therefore, a practical optimisation workflow should not only generate efficient trade-offs but also support selecting one implementable package with a clear energy–cost–CO_2 balance.

To address this setting, recent work highlights Multi Objective Particle Swarm Optimization (MOPSO) for building retrofit and design problems involving discrete options and continuous sizing. MOPSO is competitive when leader selection, archive diversity, and constraints are handled carefully [13]-[15], and PSO-based surrogate approaches have also been used to support robust search in retrofit sizing and coupled ESM effects. In parallel, Non-Dominated Sorting Genetic Algorithm II (NSGA-II) is a reference evolutionary method in buildings, and its fast non-dominated sorting, elitism, and crowding distance often yield well-spread fronts at practical runtimes [2], [3], [6]. Applications range from energy–comfort and energy–daylighting to envelope studies, and at the campus scale researchers combine urban building energy models with NSGA-II for Pareto exploration and Technique for Order of Preference by Similarity to Ideal Solution (TOPSIS) for ranking to shortlist retrofit packages under uncertainty and budget rules [5]. In addition, [9], [16], [17] establish NSGA-II's reliability for retrofit optimization, whereas [10] demonstrates improved Pareto-front diversity via multi-agent NSGA-II in challenging or many-objective settings.

Despite these advances, many optimization studies still emphasize continuous variables such as envelope parameters,

This manuscript is submitted on October 14, 2025, revised on March 9, 2026, accepted on April 1, 2026, and published on April 30, 2026.

Siti Solehah Md Ramli, Mohammad Nizam Ibrahim, Anuar Mohamad @ Ahmad, Kamarulazhar Daud, Abdul Malek Saidina Omar are from the Faculty of Electrical Engineering, Universiti Teknologi MARA Cawangan Pulau Pinang, Permatang Pauh Campus, 13500 Seberang Prai, Pulau Pinang, Malaysia.

Nor Shuhada Ibrahim is from Faculty of Innovative Design & Technology, Universiti Sultan Zainal Abidin (Unisza) Gong Badak Campus, 21300 Kuala Nerus Terengganu.

*Corresponding author
Email address: solehahramli@uitm.edu.my

HVAC setpoints, and geometry, or handle discrete choices by ranking after the optimization. By contrast, audited ESM portfolios that encode binary adoptions together with continuous sizing inside a single multi-objective formulation are less common. At the campus scale, portfolio studies with urban building energy models use NSGA-II to explore Pareto sets and then shortlist discrete retrofit packages [5].

This motivates an audited mixed-type formulation in which the catalogue of measures, caps, and unit prices is kept intact so that optimization outputs map directly to implementable proposals. This study benchmarks two widely used EMO algorithms, namely MOPSO and NSGA-II, on an audited Malaysian academic building. The ESM set mixes binary adoptions with continuous sizing, yielding a non-convex mixed-discrete search space that suits evolutionary and surrogate-assisted pipelines [2]-[5], [6]-[8], [18], [19]. Full Pareto sets are reported, followed by knee-point selection to produce actionable packages with high marginal benefit per unit cost sacrifice [20]-[22]. Economic indicators are then quantified following standard life-cycle-costing guidance [23], [24]. For carbon accounting, Malaysia's grid-emission factors from the Sustainable Energy Development Authority (SEDA) Malaysia are applied so that avoided CO_2 figures remain consistent with campus KPIs and IPMVP-style M&V [11], [12].

Facility decision-making converges on a single, budget-constrained package drawn from the audited ESM catalogue, necessitating a principled rule to collapse the Pareto set into one actionable choice. Knee-point selection provides a preference-light choice by identifying the elbow region where additional saving begins to require much higher additional cost and provides smaller gains in avoided CO_2. This study adopts a curvature-based post-hoc knee rule that is transparent and weight-free. The detailed implementation is provided in the methodology section, consistent with established curvature-based knee selection methods [25], [28], [29]. Alternative families exist, including utility-based detectors and knee-guided EMO, but these approaches introduce additional tuning or modify the generator; a post-hoc curvature rule preserves reproducibility on already-generated fronts [21], [26], [27]. Distance-to-utopia choices minimise global compromise and may miss the local elbow, whereas curvature-based logic better captures the "after-this-point, gains get expensive" narrative used to justify budgets [25], [28].

This paper contributes:

i) An audited, decision-grade ESM optimization framework. Mixed decision types, comprising continuous adoption levels and binary controls, are solved under a bi-objective trade-off between annual energy saving and investment cost, while avoided CO_2 is computed from energy saving using the fixed grid-emission factor as a carbon metric; packages are valued over 10 years using Simple Payback Period (SPP), discounted ROI, Life- Cycle Cost (LCC), and Savings-to-Investment Ratio (SIR).

ii) A curvature-based knee rule converts the cost–energy saving Pareto front into one implementable package per run, and the avoided CO_2 of the selected package is then computed using the fixed grid-emission factor.

iii) Robust comparative evidence and guidance. Thirty paired seeds with two-sided Wilcoxon tests show statistically significant between-method differences at the knee point, providing practical guidance for selecting between MOPSO and NSGA-II under audited ESM planning.

II. Case Study

This study evaluates an institutional academic building in Peninsular Malaysia, comprising five storeys with lecture rooms, classrooms, and offices, operating on standard office hours (07:30–17:30, five working days per week). A formal energy audit was conducted and used as the primary basis for site descriptors and modelling inputs. Short-term on-site measurements covering the main switchboard (MSB) and downstream distribution boards for lighting/plug/FCU, chiller power and chilled-water flow, and basic indoor air-quality and lux surveys complemented the audit to characterise subsystem loads and schedules.

Based on the energy audit, the annual electricity consumption used for benchmarking and savings attribution is 590,555 kWh/yr, established by reconciling logged subsystem shares with facility-management annual totals. Monetary conversions follow the site tariff RM 0.535/kWh (C1 + ICPT), and avoided emissions are computed using the Peninsular grid factor [11]. The auditor proposed seven ESMs spanning no-cost, low-cost, and high-cost actions: (1) tariff management; (2) awareness training; (3) occupancy/motion sensors; (4) lighting retrofit; (5) Energy Management System (EMS); (6) Building Management System (BMS); and (7) partial deployment of variable-refrigerant-flow (VRF) units to selected zones, while the existing chilled-water system is retained elsewhere. For each ESM, the audit specifies the maximum technical potential, the decision type (binary or fractional), and the associated investment cap; these inputs are adopted unchanged for the optimization, as shown in Table I. As shown in Table I, the catalogue includes one tariff-only action with no Capital Expenditure (CAPEX). It is retained for context but excluded from the optimization decision vector. Awareness Training is a non-technical behavioral measure included for completeness. Occupancy/Sensor represents low- to medium-cost controls, while Lighting refers to lamp, ballast, and driver retrofits. EMS denotes a software and metering layer, BMS provides central supervisory control, and VRF denotes a partial chiller retrofit using variable-refrigerant-flow equipment with relatively high cost. The auditor's "all-ESMs" scenario estimates 260,999.93 $kWh \cdot yr^{-1}$ savings, RM 139,634.96 annual bill savings, RM 941,525 capital cost, and 166.78 tCO_2/yr avoided under the above tariff and grid factor.

TABLE I. AUDIT-DERIVED ESM CATALOGUE USED AS OPTIMIZATION INPUTS

No	Energy Saving Measure (ESM)	Decision Type	Maximum Potential (%)	Estimated Investment Cost (RM)
1	Tariff Management	Not applicable	–	–
2	Awareness Training	Binary	1	0
3	Occupancy/Sensor	Fractional	10	7,500.00
4	Lighting Upgrade	Fractional	28	38,025.00
5	EMS	Binary	5	60,000.00
6	BMS	Binary	10	100,000.00
7	VRF System	Fractional	30	736,000.00

III. ENERGY SAVING MEASURE (ESM) OPTIMIZATION SETUP

A. Variables and Feasible Space

Optimization is defined on a mixed decision vector comprising three fractional technology variables and three binary program/control variables as given in (1):

$$x = [x_1, x_2, x_3, x_4, x_5, x_6] \tag{1}$$

where x_1 is occupancy/sensor, x_2 is lighting upgrade and x_3 is VRF system are continuous, $x_{1:3} \in [0,1]$. Meanwhile, x_4 is awareness training, x_5 is EMS, and x_6 is BMS are binary, $x_{4:6} \in \{0,1\}$. Each measure, j is capped by an audited maximum technical potential, $p_j \in [0,1]$. Realized coverage is $q_j = p_j x_j$ with bounds $0 \le q_j \le p_j$. Capital cost is computed from audited unit costs u_j as given in (2):

$$C(x) = \sum_j u_j q_j = \sum_j u_j p_j x_j \tag{2}$$

Tariff management has no CAPEX and is excluded from the decision vector. It is treated as an exogenous rate assumption used only in the economic evaluation.

B. Objectives and Sign Conventions

Two optimization objectives are considered simultaneously: maximization of annual energy saving $ES(x)$and minimization of investment cost $C(x)$. Avoided CO_2, denoted $CO_2(x)$, is computed from energy saving using the fixed grid-emission factor. For solver uniformity, maximization of annual energy saving is written as minimization of negative energy saving, as given in (3):

$$f_1(x) - ES(x) = -\big(E_{ctrl} frac(x)\big) \tag{3}$$

where $ES(x)$ is the predicted annual energy saving from the PSO-ANN baseline scaled by adopted fractions. Meanwhile the E_{ctrl} denotes the PSO-ANN baseline annual energy for the controllable end-uses targeted by the ESM catalogue which are awareness, lighting, occupancy/sensors, EMS, BMS, and VRF. Using a predicted baseline rather than the whole-facility total of 590,555 kWh/yr which is used for benchmarking confines savings to controllable loads, lets fractional decisions map smoothly to energy impact, and reduces sensitivity to short-term logger noise and schedule variability. The aggregate adoption fraction is given as in (4):

$$\begin{aligned} frac(x) = min\big(&0.10x_{\text{Occupancy/sensor}} + 0.28x_{\text{Light}} + 0.30x_{\text{VRF}} \\ &+ 0.01b_{\text{Aware}} + 0.05b_{\text{EMS}} \\ &+ 0.10b_{\text{BMS}}, (1)\big) \end{aligned} \tag{4}$$

where $x_{\text{Occupancy/sensor}}, x_{\text{Light}}, x_{\text{VRF}} \in [0,1]$ are fractional adoption variables (penetration up to their audit caps 10 %, 28 %, and 30 %, and $b_{\text{Aware}}, b_{\text{EMS}}, b_{\text{BMS}} \in \{0,1\}$ are binary decisions that add fixed increments 1 %, 5 %, and 10 %, respectively. These coefficients are obtained from the audit maximum potential in Table I. The outer $\min(\cdot\,,1)$ enforces that total adoption does not exceed 100 %. These variables represent adoption shares, not costs; capital and Operation & Maintenance (O&M) terms are handled separately in the investment-cost objective.

The resulting Pareto fronts and knee-point packages should therefore be interpreted as conditional on the present energy-savings model, namely the fixed PSO–ANN baseline for the controllable end-uses and the audit-derived linear adoption-fraction formulation used to map ESM uptake into annual energy saving. Under this modelling frame, the absolute locations of the Pareto front and the selected knee may change if an alternative surrogate, a different baseline definition, or a nonlinear interaction model among ESMs is introduced. However, because both MOPSO and NSGA-II are evaluated under the same baseline, decision-variable structure, feasibility limits, and economic assumptions, the comparative conclusions reported in this study remain internally consistent within the stated assumptions. Accordingly, the present results support relative comparison between optimizers under a common modelling frame, while broader sensitivity to alternative savings models is acknowledged as an important direction for future work.

The estimated investment cost is given in (5):

$$\begin{aligned} f_2(x) = C(x) = \; &7{,}500\, x_{\text{Sensor}} + 38{,}025\, x_{\text{Light}} \\ &+ 736{,}000\, x_{\text{VRF}} + 0.\, b_{\text{Aware}} \\ &+ 60{,}000\, b_{\text{EMS}} \; + 100{,}000\, b_{\text{BMS}} \end{aligned} \tag{5}$$

The estimated investment cost $C(x)$is a linear CAPEX model built directly from the audit entries in Table I. Fractional measures (Occupancy/Sensor, Lighting, and VRF) scale their item cost by the adoption level, $x. \in [0,1]$, while binary measures (Awareness, EMS, and BMS) contribute their full item cost when selected, $b. \in \{0,1\}$. Tariff management carries no capital outlay and is excluded. Awareness training has RM 0 CAPEX but is included for its saving or behavioural effect only.

The avoided CO_2 is given in (6) :

$$f_3(x) = -CO_2(x) = -ES(x)\gamma \tag{6}$$

where $\gamma = 0.639\ \mathrm{t}CO_2\mathrm{MWh}^{-1}$ is the Peninsular Malaysia grid emission factor (EF) [11]. Under this fixed emission factor assumption, avoided CO_2 is a linear transformation of energy saving and is therefore not an independent optimization objective. As a result, the optimization effectively reduces to a bi-objective trade-off between investment cost and energy saving, while avoided CO_2 is retained as a carbon metric to make the emissions implication of each candidate package explicit and consistent with Malaysian practice and M&V conventions [11], [12].

C. Economic Evaluation Framework

Using $ES(x)$ and $C(x)$ defined in Equation (3) and (5), each optimizer produces a non-dominated Pareto front in the energy saving–cost plane. Avoided CO_2 is computed for each solution using the fixed grid-emission factor. A single actionable solution is selected at a curvature-based knee on the energy saving–cost front. The avoided CO_2 associated with the selected solution is then computed from the energy saving. Economic performance of the knee is evaluated over a 10-year horizon with fixed assumptions: electricity tariff $T = 0.535$ RM/kWh, discount rate $r = 0.05$, and annual operation-and-maintenance fraction $f_{\mathrm{OM}} = 0.01$ of initial cost. To interpret economic attractiveness, standard life-cycle indicators are computed for the selected knee solution(s), namely SPP, discounted ROI, LCC, and SIR.

i) Simple Payback Period (SPP) is defined in (7):

$$SPP = \frac{C(x)}{ES(x)T} \tag{7}$$

where T is the electricity tariff. The result is in years. SPP is simple but ignores the time value of money and post-payback benefits.

ii) Discounted Return on Investment (ROI) over an N-year horizon is given in (8)

$$ROI_{disc}(\%) = \frac{\sum_{y=1}^{N} \frac{ES(x)\,T_y}{(1+r)^y} - \sum_{y=1}^{N} \frac{O\,\&M_y}{(1+r)^y} - C(x)}{C(x)} \times 100 \tag{8}$$

where T_y is the tariff in year y, r is the discount rate, and $O\&M_y$ is annual operation & maintenance. A positive ROI_{disc} indicates discounted benefits exceed costs. ROI > 0% indicates that discounted savings exceed the initial cost. Unlike simple ROI, discounted ROI discounts future cash flows to present value using r, so it reflects the time value of money and avoids overstating projects whose savings arrive later.

iii) Life-Cycle Cost (LCC)

Life-Cycle Cost (LCC) quantifies the discounted total cost of ownership over the analysis horizon. It combines the upfront CAPEX and the present value of all future O&M outlays, minus the present value of energy-bill savings. It indicates whether an option remains cost-effective in the long run under the assumed discount rate and tariff path.

$$LCC = C(x) + \sum_{y=1}^{N} \frac{O\&M_y}{(1+r)^y} - \sum_{y=1}^{N} \frac{ES(x)T_y}{(1+r)^y} \tag{9}$$

Lower LCC indicates better long-term economy.

iv) Savings-to-Investment Ratio (SIR)

Savings-to-Investment Ratio (SIR) measures benefit cost efficiency. It is the ratio of the present value of savings to the present value of total investment (CAPEX and O&M).

$$SIR = \frac{\sum_{y=1}^{N} \frac{ES(x)T_y}{(1+r)^y}}{C(x) + \sum_{y=1}^{N} \frac{O\&M_y}{(1+r)^y}} \tag{10}$$

SIR > 1 indicates an economically viable project.

D. Statistical Reporting

Reproducibility and interpretability are maintained by summarizing results with appropriate statistics and hypothesis tests that distinguish genuine effects from random variability. Accordingly, 30 independent seeds are run per optimizer. For each outcome, results are reported as the median (Q2) with interquartile range [Q1, Q3]. Between-optimizer differences are assessed with a two-sided paired Wilcoxon signed-rank test ($\alpha = 0.05$). The p-value, test statistic Z, and effect size r_z are reported. The effect size is given in (11):

$$r_z = \frac{Z}{\sqrt{N}}, N = 30. \tag{11}$$

where Z is the standardized test statistic from the paired Wilcoxon signed-rank test (the z-score after centering and scaling the signed-rank sum, with continuity/tie corrections as applicable). N is the number of paired observations with non-zero differences. In this study $N = 30$ unless ties reduce it. The sign of r_z indicates direction (which optimizer tends to be larger/smaller); magnitudes can be interpreted roughly as small ≈ 0.10, medium ≈ 0.30, large ≥ 0.50.

IV. Multi-Objective Optimization Methods

ESM and retrofit planning involve conflicting goals, so this section details the EMO algorithms and the curvature-based knee-selection used to produce comparable Pareto sets and one actionable package per run. Two evolutionary optimizers are considered: MOPSO and NSGA-II. Both operate under identical evaluation budgets, bounds, and feasibility repair so that differences reflect search dynamics rather than settings. Population diversity is preserved via crowding-distance archive truncation in MOPSO and crowding distance in NSGA-II, yielding comparable Pareto sets across runs. From each run's cost–energy saving Pareto front, a curvature-based knee is

identified to represent the point of maximum marginal gain per additional cost. The avoided CO_2 of the selected knee is then computed using the fixed grid-emission factor and visualized as a 3D projection.

A. Multi-Objective Particle Swarm Optimization (MOPSO)

MOPSO addresses conflicting goals by producing a set of non-dominated (Pareto-optimal) solutions rather than a single optimum. Pareto dominance underpins the external archive of current solutions that MOPSO maintains throughout the search. A Pareto-archived MOPSO is employed with leaders selected at random from the external archive and velocity clamping. For particle i at iteration t, velocity is updated by:

$$v_i^{t+1} = \omega^t v_i^t + c_1 r_1 (p_i - x_i^t) + c_2 r_2 (g_i - x_i^t) \quad (12)$$

where v_i^t is the current velocity of particle i at iteration t; ω^t is inertia weight at iteration t, c_1 and c_2 are the cognitive and social acceleration coefficients; r_1 and r_2 are the independent random numbers drawn from $U(0,1)$. The personal best p_i is the best non-dominated position visited by particle i; the guide g_i is sampled from the external archive and x_i^t is the current position of particle i at iteration t.

After the velocity update, the position is updated by:

$$x_i^{t+1} = x_i^t + v_i^{t+1} \quad (13)$$

where x_i^t is current position of particle i and v_i^{t+1} is the updated velocity from Equation (12).

To prevent divergence, each velocity component is clamped is given in (14):

$$\left|v_{ij}^{t+1}\right| \le v_{max,j} = \alpha_v (u_j - l_j), \quad \alpha_v \in (0,1] \quad (14)$$

where v_{ij}^{t+1} is the velocity of component j of particle i at iteration $t+1$; $v_{max,j}$ is the velocity clamp for component j; u_j and l_j are the upper and lower bounds of decision variable j and $\alpha \in (0,1]$ is the clamp factor controlling step size.

The inertia weight follows a linear schedule is given in (15):

$$\omega^t = \omega_{max} - \frac{\omega_{max} - \omega_{min}}{T} t \quad (15)$$

where ω_{max}, ω_{min} are the initial and final inertia weight values, T is the total number of iterations and t is the current iteration index ($0 \le t \le T$).

After each update, the decision vector is repaired to satisfy the mixed-variable structure and feasibility constraints. Fractional components are clipped to [0,1], binary components are thresholded at 0.50, and discrete components are rounded to the nearest admissible level. The external archive is updated by Pareto dominance, and when its size exceeds the predefined capacity, archive truncation is performed using a crowding-distance criterion to preserve diversity [30], [31]. Leader particles for the next iteration are then selected at random from the archive [30], [31].

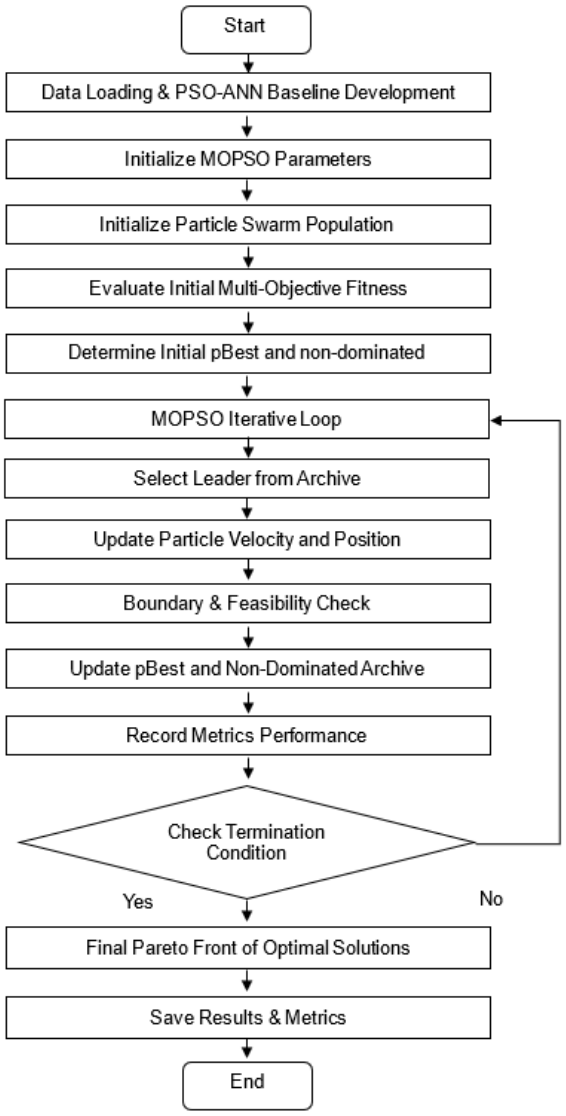

Fig.1: Flowchart of Multi-Objective Particle Swarm Optimization (MOPSO)

Fig. 1 summarizes the MOPSO workflow used for ESM optimization. A fixed PSO–ANN baseline is first developed to estimate the business-as-usual energy use. The optimizer then evaluates mixed decision vectors under the bi-objective formulation of annual energy saving and investment cost, while avoided CO_2 is computed separately from the selected knee solution using the fixed grid-emission factor. At each iteration, particle positions are updated, repaired for feasibility, and used to update the personal bests and the non-dominated archive until the stopping criterion is reached. The final archive forms the Pareto front for that run, from which the knee solution is identified.

The MOPSO hyperparameters used in this study are summarized in Table II. A swarm of 40 particles is evolved for 300 iterations with an external archive size of 40. Leaders are selected at random from the archive, and elitism is enforced through Pareto dominance with crowding-distance truncation

when the archive exceeds capacity. Positions are projected to $[0,1]$, binary entries are thresholded to $\{0,1\}$, and velocity clamping is applied in every dimension. To ensure fair comparison across runs, performance is reported using the median and interquartile range (IQR) over independent random seeds.

TABLE II. MOPSO HYPERPARAMETER CONFIGURATION AND SEARCH GRID

PARAMETER	VALUES EXPLORED
Swarm size, N	40
Max iterations, T	300
Archive size	40 (elitist; crowding-distance truncation)
Leader selection	Random selection from archive (archive truncated by crowding distance when overcapacity)
Velocity clamp	$[-0.1, ,0.1]$ (per dimension)
Position repair	Clip to $[0,1]$; binaries → threshold 0.50; discrete $x_{4:6}$→ round to $\{0,1\}$
Inertia weight, ω	{0.4,0.5…,1.5}
Acceleration coefficients , (c_1, c_2)	(0.5,0.5), (1.0,1.0), (1.0,1.5), (1.1,1.9), (1.2,1.8), (1.3,2.0), (1.4,1.7), (1.5,1.5), (1.5,1.7), (1.6,1.6), (1.7,1.4), (1.7,1.5), (1.8,1.2), (2.0,1.3), (2.0, 2.0)

B. Non-Dominated Sorting Genetic Algorithm II (NSGA-II)

NSGA-II is a widely used evolutionary multi-objective optimizer for handling conflicting objectives. In this study, a standard elitist NSGA-II is used as the comparison baseline to generate Pareto fronts under the same decision space, feasibility rules, and evaluation budget as MOPSO.

A central concept in NSGA-II is Pareto dominance. For any two solutions $u$and v, dominance is defined in (16):

$$u \prec v \iff \forall m: f_m(u) \le f_m(v) \text{ and } \exists m: f_m(u)\, f_m(v) \quad (16)$$

where u and v are candidate solutions, $f_m(\cdot)$ is the m-th objective value, and m indexes the objectives. A solution dominates another if it is no worse in all objectives and strictly better in at least one. The non-dominated set formed under this relation represents the Pareto front of trade-off solutions.

NSGA-II then applies the standard sequence of fast non-dominated sorting and crowding-distance assignment, followed by binary tournament selection, simulated binary crossover (SBX), polynomial mutation, and elitist environmental selection [13], [32]. Since these operators are not modified in this study, only the main workflow and problem-specific implementation details are summarized here. After variation, each offspring is repaired to satisfy the mixed decision structure by clipping continuous variables to $[0,1]$ and rounding binary/discrete entries to the nearest admissible level.

Elitism is enforced by merging the parent and offspring populations is given in (17):

$$R_t = P_t \cup Q_t \quad (17)$$

where P_t is the parent population at generation t, Q_t is the offspring population, and R_t is the combined population used for environmental selection. The next generation is then formed by retaining better Pareto ranks first and, when truncation is required within the last accepted front, preferring solutions with larger crowding distance to preserve diversity [33], [34].

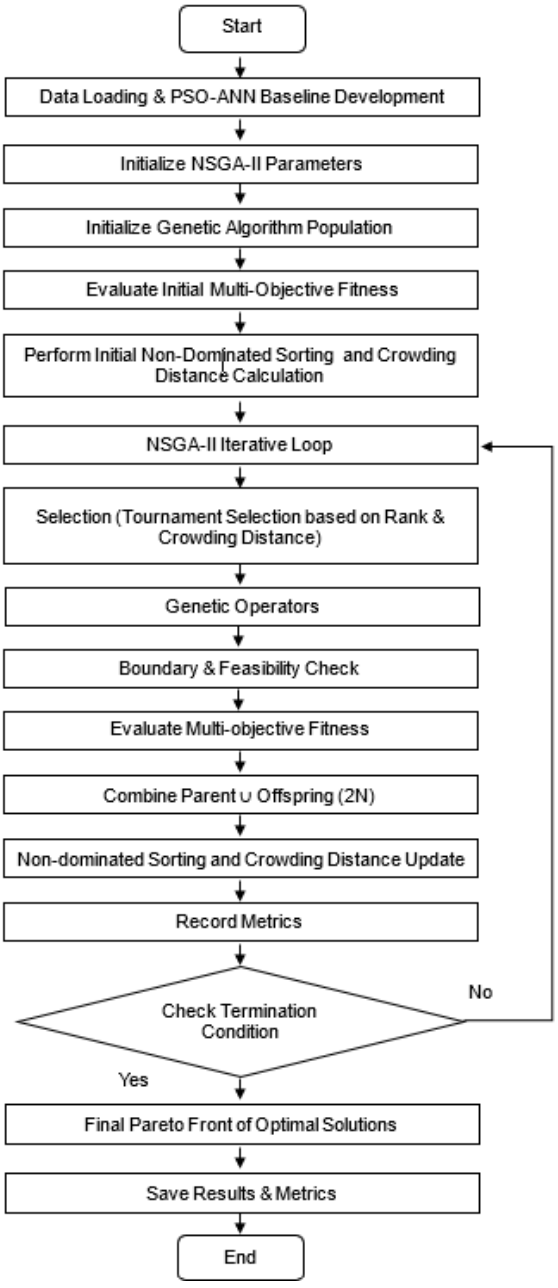

Fig.2. Flowchart of Non-Dominated Sorting Genetic Algorithm II (NSGA-II)

Fig. 2 summarizes the NSGA-II workflow used for ESM optimization. Mixed decision variables represent continuous adoption levels for occupancy/sensors, lighting, and VRF, together with binary selections for awareness, EMS, and BMS. The algorithm evaluates the same bi-objective formulation of annual energy saving and investment cost as used in MOPSO, while avoided CO_2 is computed separately from energy saving using the fixed grid-emission factor. At each generation, the population is ranked, selected, varied, repaired for feasibility,

and merged with its offspring until the stopping criterion is reached. The final rank-1 set forms the Pareto front for that run, from which the curvature-based knee solution is identified.

As with MOPSO, hyperparameters for NSGA-II regulate the exploration–exploitation balance and front diversity; documenting their ranges ensures reproducibility and a fair comparison. Table III summarizes the NSGA-II configuration used in this study. An elitist, diversity-preserving scheme is adopted with a fixed population size of 40 and 300 generations. A grid search explores crossover probability $P_c \in \{0.80,0.90,1.00\}$ and mutation probability $P_m \in \{0.05,0.10,0.15\}$, together with the SBX and polynomial-mutation distribution indices $\eta_c, \eta_m \in \{15,18,20,21,24,25,27,30\}$. After variation, decision vectors are repaired by clipping continuous variables to $[0,1]$ and rounding the binary entries $x_{4:6} \to \{0,1\}$. To quantify robustness, each hyperparameter setting is evaluated across 30 random seeds, and performance is summarized as median and interquartile range (IQR) across independent seeds.

TABLE III. NSGA-II HYPERPARAMETER CONFIGURATION AND SEARCH GRID

PARAMETER	VALUES EXPLORED IN GRID
Population size, N	40
Maximum generations, G	300
Crossover probability, P_c	0.80, 0.90, 1.00
Mutation probability, P_m	0.05, 0.10, 0.15
SBX distribution index, η_c	15, 18, 20, 21, 24, 25, 27, 30
Mutation distribution index, η_m	15, 18, 20, 21, 24, 25, 27,30
Random Seeds	1:30

C. Knee Point Detection

The Pareto set contains many admissible trade-offs among annual energy saving, investment cost, and avoided CO_2 emissions. To obtain a single decision-ready solution from each run without imposing subjective weights, a curvature-based knee is selected from the non-dominated front. In practice, the knee is the elbow point where further energy saving requires much higher additional investment, with smaller gains in avoided CO_2 emissions.

Let the non-dominated solutions be min–max normalised and ordered by the energy-saving objective f_1 to form a consistent traversal along the front. For each consecutive pair of points, the forward slope is computed as the Euclidean change in the (f_2, f_3) plane per unit change along the ordered f_1 axis, is given in (18):

$$s_i = \frac{\| [f_2,f_3]_{i+1} - [f_2,f_3]_i \|_2}{| f_{1,i+1} - f_{1,i} |}, i = 1, \dots, n-1 \quad (18)$$

where $f_1 = -ES(x)$, $f_2 = C(x)$, and $f_3 = CO_2(x)$; i denotes the i-th point in the sorted list; $\|\cdot\|_2$ is the Euclidean norm; and n is the number of non-dominated points in the ordered front.

A curvature proxy is computed as the absolute change between successive slopes is given in (19):

$$k_i = | s_{i+1} - s_i |, i = 1, \dots, n-2 \quad (19)$$

where i indexes the interior points used to compute successive slope changes. The knee is selected as the solution corresponding to the maximum k_i along the ordered front, indicating the point where the trade-off steepens most sharply, and is carried forward for the comparative economic evaluation.

In this study, the reported knee should be interpreted as an operational knee defined by the adopted curvature-based rule on the ordered and normalized Pareto front, rather than as a claim of universal mathematical uniqueness for every noisy front realization. Its practical stability is assessed empirically through 30 independent random seeds per optimizer, with the resulting knee-point outcomes summarized using median, interquartile range, and paired nonparametric significance tests. This design allows the study to evaluate whether the selected knee remains decision-relevant and comparatively stable across stochastic runs under a fixed detection rule. Sensitivity to alternative knee-identification methods, such as utility-based, distance-to-reference, or knee-guided evolutionary approaches, is not thoroughly tested here and is therefore acknowledged as a valuable direction for future work.

IV. RESULTS AND DISCUSSION

This subsection reports the optimization outcomes obtained with MOPSO and NSGA-II. Results are presented to illustrate the attainable trade-offs between annual energy saving and investment cost, with avoided CO_2 shown as the corresponding carbon metric under the fixed grid-emission factor.

A. Multi-Objective Particle Swarm Optimization (MOPSO)

Fig. 3 presents a 2D projection of the MOPSO Pareto front in the cost–saving plane, showing the trade-off between annual energy saving (kWh/year) and implementation cost (RM). Grey markers pool the non-dominated solutions aggregated across 30 independent runs, providing the overall spread of achievable trade-offs. Blue markers highlight a representative median run, selected as the run whose knee has an LCC closest to the cross-run median, which provides a clean visual of one typical frontier within the wider ensemble of approximately 1,200 pooled solutions. The red marker denotes the selected knee solution used for the subsequent economic evaluation. The knee corresponds to 54,473.9 kWh/year at RM 119,134, and lies at the elbow of the Pareto curve, where additional savings beyond this level require a substantially higher CAPEX per incremental kWh saved. Hence, it represents a practical and implementable compromise for decision-making.

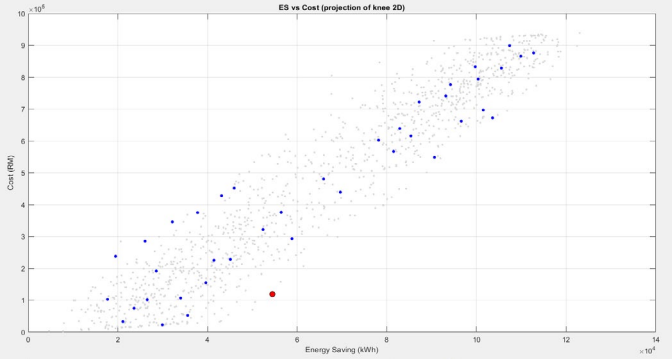

Fig. 3. 2D projection of the MOPSO Pareto front (investment cost vs energy saving) with the selected knee used for economic evaluation.

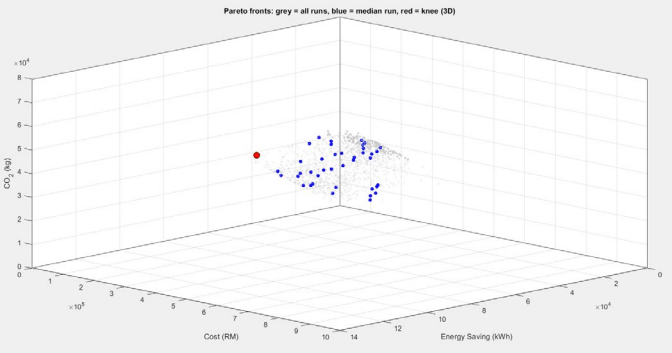

Fig. 4. 3D Pareto front for investment cost, energy saving, and CO_2 avoidance using MOPSO

Fig. 4 displays the corresponding 3D Pareto front from MOPSO with investment cost, annual energy saving, and avoided CO_2 emissions. Because avoided CO_2 scales linearly with energy saving under the fixed grid-emission factor, the non-dominated set aligns approximately on a tilted plane in the 3D space. Grey markers pool the non-dominated solutions across runs, blue markers show the same median run as in Fig. 3, and the red marker indicates the selected knee. This knee achieves 54,473.9 kWh/year, costs RM 119,134, and avoids 34.81 tCO_2/year. The associated avoided CO_2 emissions quantify the environmental benefit of the selected knee package under the stated grid-emission factor, supporting carbon-oriented reporting alongside economic metrics.

Table IV presents the optimized ESM fractions at the Pareto knee and their resulting effective coverage (%) under the MOPSO approach. Each optimized fraction is mapped to an on-site deployment percentage by multiplying the measure's audited maximum potential by its optimized fraction, reported to two decimals. Awareness training is not adopted, yielding 0 % effective coverage. Occupancy/sensor controls are applied at a fraction of 0.913 on a 10 % potential, giving 9.13 % effective coverage. Lighting upgrade is deployed at a fraction of 0.837 on a 28 % potential, yielding 23.44 % effective coverage, the largest technical contribution at the knee. EMS and BMS are not selected, so both report 0 % coverage. VRF system is used sparingly; a fraction of 0.109 on a 30 % potential corresponds to 3.27 % effective coverage.

Overall, the MOPSO knee concentrates adoption on occupancy/sensor controls and lighting, excludes EMS and BMS, and limits VRF to targeted zones. This allocation prioritizes measures with strong savings per unit cost, yielding lower upfront expenditure and a faster simple payback while retaining meaningful energy and CO_2 reductions consistent with the relative financial advantage observed for the MOPSO knee.

TABLE IV. OPTIMIZED ESM FRACTIONS AT THE PARETO KNEE AND THEIR EFFECTIVE COVERAGE FOR MOPSO

No	Energy Saving Measures (ESM)	Maximum Potential (%)	Fraction Used	Effective Coverage (%)
2	Awareness Training	1	0	0
3	Occupancy/Sensor	10	0.913	9.13
4	Lighting Upgrade	28	0.837	23.45
5	Energy Management System	5	0	0
6	Building Management System	10	0	0
7	VRF System	30	0.109	3.28

B. Non-Dominated Sorting Genetic Algorithm II (NSGA-II)

For comparison under identical settings, the NSGA-II results are presented as similarly structured Pareto frontiers in both 2D and 3D views. Figure 5 presents a 2D projection of the NSGA-II Pareto front in the cost–saving plane, showing the trade-off between annual energy saving (kWh/year) and implementation cost (RM). Grey markers pool the non-dominated solutions aggregated across 30 independent runs, providing the overall spread of achievable trade-offs. Blue markers highlight a representative median run, selected as the run whose knee has an LCC closest to the cross-run median, which provides a clean visual of one typical frontier within the wider ensemble of approximately 1,200 pooled solutions. The red marker denotes the selected knee solution used for the subsequent economic evaluation. In this 2D view, the knee corresponds to 60,271.9 kWh/year at RM 170,866. Compared with the MOPSO knee, the NSGA-II knee is shifted toward higher energy saving but requires a higher investment, which is reflected in the comparative economic indicators.

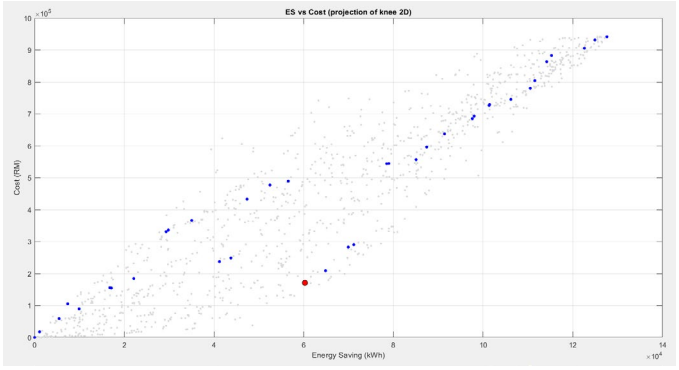

Fig. 5. 2D projection of the NSGA-II Pareto front (investment cost vs energy saving) with the selected knee used for economic evaluation.

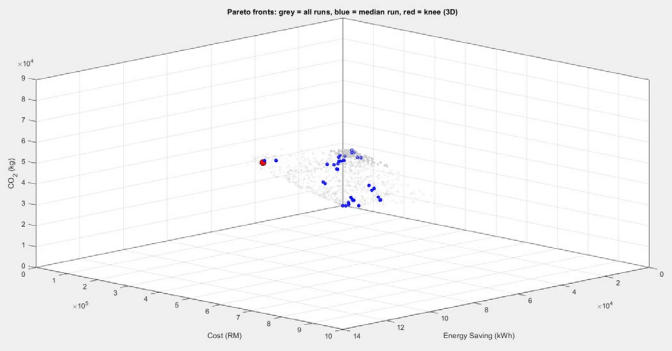

Fig. 6. 3D Pareto front for investment cost, energy saving, and CO_2 avoidance using NSGA-II

Fig. 6 displays the corresponding 3D Pareto front from NSGA-II with investment cost, annual energy saving, and avoided CO_2 emissions. Because avoided CO_2 emissions scale linearly with energy saving under the fixed grid-emission factor, the non-dominated set aligns approximately on a tilted plane in the 3D space. Grey markers pool the non-dominated solutions across runs, blue markers show the same median run as in Fig. 5, and the red marker indicates the selected knee. This knee achieves 60,271.9 kWh/year, costs RM 170,866, and avoids 38.51 tCO_2/year, and is carried forward for the economic assessment. The avoided CO_2 value quantifies the annual carbon reduction delivered by the selected knee package under the stated grid-emission factor.

Table V presents the optimized ESM fractions at the Pareto knee and their resulting effective coverage (%) under the NSGA-II approach. Awareness training is fully adopted, yielding 1.00 % effective coverage. Meanwhile the occupancy/sensor controls are applied at a fraction of 0.367 on a 10 % potential, giving 3.67 % effective coverage. Lighting upgrade is deployed at a fraction of 0.840 on a 28 % potential, yielding 23.53 % effective coverage which is the largest technical contribution at the knee. EMS is not selected. BMS is fully enabled, producing 10 % effective coverage. Finally, the VRF system is used minimally, with a fraction of 0.049 on a 30 % potential, corresponding to 1.47 % effective coverage. Overall, the NSGA-II knee emphasizes full supervisory control via BMS and deep lighting upgrades, with moderate occupancy/sensor deployment, minimal VRF, and no EMS.

TABLE V. OPTIMIZED ESM FRACTIONS AT THE PARETO KNEE AND THEIR EFFECTIVE COVERAGE FOR NSGA-II

No	Energy Saving Measures (ESM)	Maximum Potential (%)	Fraction Used	Effective Coverage (%)
2	Awareness Training	1	1.000	1.00
3	Occupancy/Sensor	10	0.367	3.67
4	Lighting Upgrade	28	0.840	23.53
5	Energy Management System	5	0	0
6	Building Management System	10	1.000	10.00
7	VRF System	30	0.049	1.47

The stronger economic performance of the MOPSO knee is mainly driven by the cost structure of its selected package. MOPSO avoids fixed-cost supervisory layers, including BMS and EMS, and concentrates adoption on lower-cost, high-yield measures such as occupancy-based controls, sensors, and lighting upgrades. In contrast, NSGA-II enables BMS and adopts additional measures that raise the upfront CAPEX. As a result, NSGA-II delivers higher annual saving, 60,271.9 versus 54,473.9 kWh/year, but at substantially higher investment, RM 170,866 versus RM 119,134, which explains the economic differences observed in Table VI.

C. Knee-Point Economic Comparison

Knee-point economics were summarized across 30 paired runs to assess cross-method consistency. For the MOPSO knees, the median (IQR) simple payback was 2.25 yr (Q1- Q3: 1.57 - 2.83 yr), with a discounted ROI of 235 % (165 - 385 %). LCC was negative at −RM 92.8k (−107 k to −79.8 k), and SIR was 3.18 (2.53 - 4.58). These quartiles indicate rapid cost recovery and strong net present value, with relatively tight dispersion that signals stable performance across replicates.

For NSGA-II, the knees remained economically viable but with weaker central tendency and wider spread: median payback 3.54 yr (2.34 - 5.30 yr), discounted ROI 110 % (38 -222 %), LCC −RM 62.6k (−75.9k −29.1k), and SIR 2.03 (1.35–3.06). The broader upper quartile in SPP and lower quartiles in discounted ROI/LCC point to greater variability and a heavier tail toward less favourable outcomes. Overall, while both optimizers yield cost-effective knees, MOPSO delivers faster payback, larger ROI, more negative LCC, and higher SIR with tighter IQRs, indicating more consistent economic gains across runs.

TABLE VI. KNEE-POINT ECONOMIC OUTCOMES ACROSS 30 PAIRED RUNS: MEDIANS (Q2) AND QUARTILES (Q1, Q3).

Metric	MOPSO			NSGA-II		
	Med	Q1	Q3	Med	Q1	Q3
SPP (Yr)	2.25	1.57	2.83	3.54	2.34	5.3
Disc ROI (%)	235.2	165.1	385.3	110.4	38.0	222.3
LCC (RM)	−92,8 16.00	−107, 670.0	−79,7 99.00	−62,6 14.00	−75,93 5.00	−29,1 46.00
SIR	3.18	2.53	4.58	2.03	1.35	3.06

Across 30 paired runs, the two-sided Wilcoxon signed-rank tests at the knee indicate statistically significant between-method differences for all four economic indicators, SPP, discounted ROI, LCC, and SIR (all $p \leq 6.64\times10^{-4}$). These p-values show that the null hypothesis of equal medians can be rejected consistently, implying that the optimizers do not yield indistinguishable knee-point economics under identical seeds and data. The smallest p-value occurs for LCC (4.07×10^{-5}), suggesting particularly strong separation in LCC performance at the selected knee.

Effect sizes, reported as r_z, range from 0.621 to 0.749, which fall in the "large" range according to common benchmarks for non-parametric r (≈ 0.1 small, 0.3 medium, 0.5 large). The largest shift is again observed for LCC ($r_z = 0.749$), followed by SPP ($r_z = 0.704$), with ROI and SIR showing similarly substantial effects ($r_z = 0.621$). Together, these results indicate not only statistical significance but also practical significance: the choice of optimizer materially changes the knee-point

economics across all metrics, with the most pronounced impact on total LCC and SPP.

TABLE VII. PAIRED WILCOXON SIGNED-RANK TESTS AT THE KNEE (TWO-SIDED) WITH EFFECT SIZE

Metric	P-VALUES	r_z
SPP (Yr)	1.15×10^{-4}	0.704
Disc ROI (%)	6.64×10^{-4}	0.621
LCC (RM)	4.07×10^{-5}	0.749
SIR (–)	6.64×10^{-4}	0.621

D. Auditor Benchmark vs Optimized Knees

Under a common unit-price basis, the auditor's package is compared with the knee-point solutions from MOPSO and NSGA-II; tariff management is exogenous, has no CAPEX, and is excluded from the decision vector (not mapped to technical savings $ES(x)$). Both knees slash capital outlay relative to the auditor's RM 941,525 proposal to RM 119,133.83 with MOPSO and RM 170,865.67 with NSGA-II, yet still deliver material annual savings of 54,473.88 - 60,271.95 kWh yr^{-1} and avoid around 34.81 - 38.51 tCO_2/yr. The economic response is markedly stronger at the knees: simple payback improves from 6.74 yr (auditor) to 2.25 yr (MOPSO) and 3.54 yr (NSGA-II). Discounted ROI rises from 6.8 % to 235.24 % and 110.43 %, respectively; SIR increases from 1.06 to 3.18 and 2.03. Consistent with these gains, the LCC is strongly favourable at the knees (MOPSO -RM 92,816, NSGA-II -RM 62,614) compared with the auditor's positive LCC.

Between the algorithms, NSGA-II yields the larger technical impact with higher annual energy saving (60,272 kWh/yr) and greater CO_2 avoidance (38.51 t CO_2 /yr) but requires the higher investment cost. MOPSO, in contrast, offers the stronger financial profile at a much lower CAPEX: it achieves the shortest payback (2.25 yr), the highest discounted ROI (235.24 %), the largest SIR (3.18), and the most favourable LCC (-RM 92,816). In practical terms, the MOPSO knee is the decision-ready option when budget discipline and rapid cost recovery are prioritised, whereas the NSGA-II knee is attractive for stakeholders willing to invest more upfront to secure slightly higher annual savings and emissions abatement.

TABLE VIII. ECONOMIC PERFORMANCE COMPARISON BETWEEN THE AUDITOR'S PROPOSAL AND THE KNEE-POINT SOLUTIONS (MOPSO AND NSGA-II).

Item	AUDITOR	MOPSO	NSGA-II
Baseline energy (kWh/yr)	590,555.00	590,555.00	590,555.00
Annual energy saved (kWh/yr)	260,999.90	54,473.88	60,271.95
Energy savings relative to baseline (%)	44.20	9.22	10.21
Capital investment (RM)	941,525.00	119,133.83	170,865.67
Simple payback, SPP (yr)	6.74	2.25	3.54
Discounted ROI (%)	6.80	235.24	110.43
LCC (RM)	−63,996.98	−92,816.00	−62,614.00
SIR	1.06	3.18	2.03
CO_2 avoided (t/yr)	166.78	34.81	38.51

V. CONCLUSION

This study benchmarked two evolutionary multi-objective optimizers, namely MOPSO and NSGA-II, for selecting audited, decision-ready ESM portfolios under a common unit-price basis. Curvature-based knee selection converts full Pareto sets of audited ESM options into implementable retrofit packages with transparent trade-offs. Under identical assumptions, both MOPSO and NSGA-II produce viable knees; however, the MOPSO knee exhibits a stronger financial profile, while the NSGA-II knee achieves marginally higher technical savings at a higher outlay. Consistency across repeated seeds together with paired nonparametric tests indicates that optimizer choice materially shifts knee-point economics rather than yielding interchangeable outcomes. For capital-constrained decision contexts, MOPSO offers a practical default; where slightly higher annual savings and abatement are prioritized despite added investment, NSGA-II remains credible. Beyond the algorithmic comparison, the knee-oriented protocol furnishes audit-grade, budget-ready shortlists without collapsing the multi-objective structure into a single composite score, thereby preserving interpretability for institutional stakeholders and aligning with procurement realities.

The proposed framework is generalizable at the workflow level to other audited buildings because its core stages remain the same: definition of a feasible ESM catalogue, development of a building-specific baseline or savings model, Pareto-front generation under multiple objectives, knee-based reduction to one decision-ready package, and life-cycle economic screening. However, transferability does not imply that all model components can be reused unchanged. For a different building, ESM catalogue, or economic context, the baseline predictor, audited technical potentials, unit costs, tariff structure, discount rate, grid-emission factor, and any site-specific operational constraints should be re-calibrated before optimization. Hence, the overall optimization procedure can be applied to other cases, but the surrogate model and techno-economic inputs still need to be adjusted for each building and economic scenario.

The approach is reproducible under the stated unit-price basis, grid-emission factor, and life-cycle evaluation settings.

These outcomes substantiate the paper's contributions by yielding implementable packages and robust comparative evidence to guide method selection. Future work can extend along three axes: (i) robustness to tariff dynamics, discount-rate scenarios, and evolving grid factors; (ii) richer control-layer modelling (such as sensor-driven schedules and supervisory logic) to capture interactive effects among measures; and (iii) adaptive optimizers such as RL-assisted MOPSO or NSGA variants to accelerate convergence while preserving front diversity. Together, these directions would strengthen the policy relevance of knee-based ESM selection for campuses and public assets.

ACKNOWLEDGMENT

The authors gratefully acknowledge Universiti Teknologi MARA and the Faculty of Electrical Engineering, UiTM Cawangan Pulau Pinang, for support in the preparation and publication of this manuscript.

REFERENCES

[1] UNEP/GlobalABC, "Global status report for buildings and construction 2024/2025," 2025. [Online]. Available:

https://www.unep.org/resources/report/global-status-report-buildings-and-construction-20242025

[2] A. Wang, Y. Xiao, C. Liu, Y. Zhao, and S. Sun, "Multi-objective optimization of building energy consumption and thermal comfort based on SVR-NSGA-II," Case Stud. Therm. Eng., vol. 63, Art. no. 105368, 2024, doi: 10.1016/j.csite.2024.105368.

[3] C. Wu, H. Pan, Z. Luo, C. Liu, and H. Huang, "Multi-objective optimization of residential building energy consumption, daylighting, and thermal comfort based on BO-XGBoost–NSGA-II," Build. Environ., vol. 254, Art. no. 111386, 2024, doi: 10.1016/j.buildenv.2024.111386.

[4] E. Kabiri and N. Maftouni, "Multiple objective energy optimization of a trade center building based on genetic algorithm using ecological materials," Sci. Rep., vol. 14, Art. no. 9366, 2024, doi: 10.1038/s41598-024-58515-8.

[5] L. Luo, H. Wei, Y. Lin, and Y. Sun, "Multi-objective optimal energy-efficient retrofit determination using hybrid urban building energy model: Considering uncertainties between models," Build. Simul., vol. 18, pp. 183–206, 2025, doi: 10.1007/s12273-024-1206-6.

[6] P. Shen, J. Chen, C. Shao, and Q. Ma, "Building energy retrofit optimization considering future climate and decision-making under various mindsets," J. Build. Eng., vol. 96, Art. no. 110422, 2024, doi: 10.1016/j.jobe.2024.110422.

[7] E. Markarian, O. R. Rethnam, A. Thomas, and E. Azar, "Informing building retrofits at low computational costs: A multi-objective optimisation using machine learning surrogates of building performance simulation models," J. Build. Perform. Simul., 2024, doi: 10.1080/19401493.2024.2384487.

[8] A. S. Cruz, L. R. Caldas, V. M. Mendes, J. C. Mendes, and L. E. G. Bastos, "Multi-objective optimization based on surrogate models for sustainable building design: A systematic literature review," Build. Environ., vol. 266, Art. no. 112147, 2024, doi: 10.1016/j.buildenv.2024.112147.

[9] K. Alexakis, V. Benekis, P. Kokkinakos, and D. Askounis, "Genetic algorithm-based multi-objective optimisation for energy-efficient building retrofitting: A systematic review," Energy Build., vol. 328, Art. no. 115216, 2024, doi: 10.1016/j.enbuild.2024.115216.

[10] Z. Zhang, "Multi-objective optimization method for building energy-efficient design based on multi-agent-assisted NSGA-II," Energy Inform., vol. 7, Art. no. 90, 2024, doi: 10.1186/s42162-024-00394-4.

[11] Sustainable Energy Development Authority (SEDA) Malaysia, "CO2 Avoidance," Statistics & Monitoring. [Online]. Available: https://www.seda.gov.my/statistics-monitoring/co2-avoidance/. Accessed: Oct. 10, 2025.

[12] Efficiency Valuation Organization (EVO), International Performance Measurement and Verification Protocol (IPMVP): Volume I — Concepts and Options for Determining Energy and Water Savings (EVO 10000-1:2012), 2012. [Online]. Available: https://www.eeperformance.org/uploads/8/6/5/0/8650231/ipmvp_volume_i__2012.pdf

[13] H. Ma, Y. Zhang, S. Sun, T. Liu, and Y. Shan, "A comprehensive survey on NSGA-II for multi-objective optimization and applications," Artif. Intell. Rev., vol. 56, no. 12, pp. 15217–15270, 2023, doi: 10.1007/s10462-023-10526-z.

[14] S. E. Aslay, "Building energy prediction model with AI-based PSO-ANN approach integrating architectural and HVAC processes," Build. Environ., vol. 282, Art. no. 113305, 2025, doi: 10.1016/j.buildenv.2025.113305.

[15] R. Shan, X. Jia, X. Su, Q. Xu, H. Ning, and J. Zhang, "AI-driven multi-objective optimization and decision-making for urban building energy retrofit: A systematic review," Appl. Sci., vol. 15, no. 16, Art. no. 8944, 2025, doi: 10.3390/app15168944.

[16] I. Costa-Carrapiço, R. Raslan, and J. Neila, "A systematic review of genetic algorithm-based multi-objective optimisation for building retrofitting strategies towards energy efficiency," Energy Build., vol. 210, Art. no. 109690, 2020, doi: 10.1016/j.enbuild.2019.109690.

[17] H. Wei, Y. Jiao, Z. Wang, W. Wang, and T. Zhang, "Optimal retrofitting scenarios of multi-objective energy-efficient historic building under different national goals integrating energy simulation, reduced order modelling and NSGA-II algorithm," Build. Simul., 2024, doi: 10.1007/s12273-024-1122-9.

[18] N. Shirzadi, M. Rezaei, and H. R. Seyedhosseini, "Surrogate modeling for building design: Energy and cost," Buildings, vol. 15, no. 13, Art. no. 2361, 2025, doi: 10.3390/buildings15132361.

[19] M. M. Saad and U. Eicker, "Developing surrogate models for holistic building retrofit optimization with multi-criteria decision-making support," Energy Build., vol. 348, Art. no. 116358, 2025, doi: 10.1016/j.enbuild.2025.116358.

[20] M. Antunes, T. Estro, P. Bhandari, A. Gandhi, G. Kuenning, Y. Liu, C. Waldspurger, A. Wildani, and E. Zadok, "Kneeliverse: A universal knee-detection library for performance curves," SoftwareX, vol. 30, Art. no. 102161, 2025, doi: 10.1016/j.softx.2025.102161.

[21] K. Li, H. Nie, H. Gao, and X. Yao, "Knee point identification based on trade-off utility (KPITU)," arXiv, 2020. [Online]. Available: https://arxiv.org/abs/2005.11600

[22] G. Li, S. Wang, and X. Yao, "A RadViz method with knee-point information for many-objective optimization (KRadViz)," Appl. Soft Comput., vol. 175, Art. no. 113064, 2025, doi: 10.1016/j.asoc.2025.113064.

[23] U.S. National Institute of Standards and Technology (NIST), Handbook 135: Life-Cycle Costing Manual for the Federal Energy Management Program, 2023 ed., Gaithersburg, MD, USA, 2023. [Online]. Available: https://www.nist.gov/services-resources/software/building-life-cycle-cost-programs

[24] U.S. Department of Energy, Federal Energy Management Program (FEMP), "Building life-cycle cost (BLCC) programs," 2024. [Online]. Available: https://www.energy.gov/femp/building-life-cycle-cost-programs

[25] K. Deb and S. Gupta, "Understanding knee points in bicriteria problems and their implications as preferred solution principles," Engineering Optimization, vol. 43, no. 11, pp. 1175–1204, 2011, doi: 10.1080/0305215X.2010.548863.

[26] X. Zhang, Y. Tian, and Y. Jin, "A Knee Point-Driven Evolutionary Algorithm for Many-Objective Optimization," IEEE Transactions on Evolutionary Computation, vol. 19, no. 6, pp. 761–776, 2015, doi: 10.1109/TEVC.2014.2378512.

[27] L. Rachmawati and D. Srinivasan, "Multiobjective Evolutionary Algorithm with Controllable Focus on the Knees of the Pareto Front," IEEE Transactions on Evolutionary Computation, vol. 13, no. 4, pp. 810–824, 2009, doi: 10.1109/TEVC.2009.2017515.

[28] P. K. Shukla, M. A. Braun, and H. Schmeck, "Theory and Algorithms for Finding Knees," in Evolutionary Multi-Criterion Optimization (EMO 2013), LNCS 7811, Springer, pp. 156–170, 2013, doi: 10.1007/978-3-642-37140-0_15.

[29] J. Lee and M. Mitici, "Multi-objective design of aircraft maintenance using Gaussian process learning and adaptive sampling," Reliability Engineering & System Safety, vol. 218, 108123, 2022, doi: 10.1016/j.ress.2021.108123.

[30] W. Zou, H. Xu, C. Chen, and C. Wu, "An enhanced MOPSO algorithm for multi-objective UAV path planning in mountainous environments," Symmetry, vol. 17, no. 11, Art. no. 1890, 2025, doi: 10.3390/sym17111890.

[31] A. J. Nebro, M. López-Ibáñez, J. García-Nieto, and C. A. Coello Coello, "On the automatic design of multi-objective particle swarm optimizers: experimentation and analysis," Swarm Intelligence, vol. 18, pp. 105–139, 2024, doi: 10.1007/s11721-023-00227-2.

[32] A. B. Katkar and H. T. Jadhav, "Meta-Strategy Epsilon-Dominance Co-operative Mechanism for Renewable-Integrated Multi-objective Optimal Power Flow Using Hybrid Artificial Bee Colony and NSGA-II Algorithm," Human-Centric Intelligent Systems, vol. 5, pp. 595–627, 2025, doi: 10.1007/s44230-025-00119-0.

[33] B. Doerr, T. Ivan, and M. S. Krejca, "Speeding Up the NSGA-II With a Simple Tie-Breaking Rule," Proc. AAAI Conf. Artif. Intell., vol. 39, no. 25, pp. 26964–26972, 2025, doi: 10.1609/aaai.v39i25.34902.

[34] X. Wu, Z. Chen, T. Liu, H. Song, Z. Wang, and W. Shi, "Improved NSGA-II and its application in BIW structure optimization," Adv. Mech. Eng., vol. 15, no. 2, Art. no. 16878132221150588, 2023, doi: 10.1177/16878132221150588.